10.21608/adjc.2023.176733.1199 Advanced Dental Journal
Volume 5 (2023) | Issue 1| Pages 67 - 78

Original Article

Antibacterial Activity and Fluoride Release of Nanochitosan-modified Glass Ionomer Compared to Conventional Cement: In Vitro Study

Aisha Abd-Elaziz Labib[1], Sabry Abd-Elhameed El-Korashy[2], Nehal Abou Raya[3], Taheya Moussa[3]

[1] Dentist at Ministry of Health.
[2] Inorganic Chemistry Department, Faculty of Science, Suez Canal University.
[3] Biomaterials Department, Faculty of Dentistry, Cairo University.

Email: nl.abouraya@dentistry.cu.edu.eg

ABSTRACT

Aim: The present study aimed to prepare chitosan nanoparticles, characterize it, and study the setting reaction of conventional GIC using Fourrier Transform Infra-red spectroscopy after adding 10% chitosan nanoparticles to the powder to enhance its antibacterial activity. The antibacterial effect against *Streptococcus mutans* and fluoride ion release were investigated.

Methodology: Nanoparticles of chitosan were produced by ionic gelation method and their size was determined by TEM. FTIR analysis was done for conventional GIC and nanochitosan-modified GIC groups. Direct contact test determined antibacterial activity while an ion-selective electrode and analyzer measured fluoride ion release in ppm where n=9 for each test.

Results: TEM revealed that the size of chitosan nanoparticles was 19-47 nm. FTIR spectrographs revealed that nanochitosan did not interfere with the setting reaction of conventional GIC and interaction occurred between NH_2 in chitosan with carboxyl and hydroxyl functional groups of conventional glass ionomer cement. Nanochitosan-modified GIC showed higher antibacterial activity and significantly higher mean values of fluoride ion release compared to the conventional GIC group.

Conclusion: Adding 10% w/w of chitosan nanoparticles to conventional GIC enhanced its antibacterial activity against *Streptococcus mutans* and fluoride ion release. Therefore, it can be considered as a promising additive to GIC to promote its anticariogenicity.

Keywords: Glass ionomer cement, chitosan nanoparticles, chitosan modified glass ionomer cement, antibacterial, fluoride release

Introduction

Glass ionomer cements (GICs) are considered the most appropriate restorative material for Atraumatic Restorative Treatment (ART) due to their biological, physical and chemical properties increasing the demand for this material in developing countries. GICs set by an acid-base reaction between calcium fluoro-alumino-silicate glass and polyacrylic acid. It exhibits recharging and fluoride release properties, adhesion to tooth tissue, compatible thermal expansion, biocompatibility and anticariogenic/antibacterial properties ((Ibrahim et al. 2015; Senthil Kumar et al. 2017; LIMA et al. 2018; Nishantine et al. 2022). Fluoride release of GIC contributes to its anticariogenicity and remineralization of damaged

hard dental tissues through ion exchange without hampering the integrity of the cement matrix. The release pattern is characterized by an early burst (initial rapid release) that increases in acidic conditions followed by slower long-term release as GIC acts as a reservoir for fluoride (Suprastiwi and Id 2010; Najeeb et al. 2016; Tiwari et al. 2016).

Streptoccous mutans is considered the primary causative microorganism of dental caries and its recurrence leading to restoration failure. Fluoride release from GIC contributes to antibacterial property (Palenik et al. 1992; Tiwari et al. 2016). Fluoride antibacterial action can be explained by several theories: (1) interfering with bacterial metabolism by inhibition of enolase (a glycolytic enzyme) and ATPase thus inhibiting acids produced by bacteria and glucans; (2) affecting intracellular or plaque-associated enzymes such as acid phosphatase, pyrophosphatase, peroxidase, and catalase; (3) adhesion of positively charged fluoride ions to bacterial cell walls exerting bacteriostatic or bactericidal actions without causing bacterial resistance that can result from antibiotics (Palenik et al. 1992a; Tiwari et al. 2016; Wassel and Khattab 2017).

Nevertheless, antibacterial effect of GIC is deficient which evoked the need to modify the material without adversely affecting its properties, fluoride release, and adhesion to the tooth ((Ibrahim et al. 2015; Najeeb et al. 2016; Tiwari et al. 2016; Debnath et al. 2017; Senthil Kumar et al. 2017). Therefore, several trials of adding synthetic or natural antimicrobial agents to GIC were conducted. Synthetic products such as *Chlorhexidine (CHX)* was added to GIC ((Ibrahim et al. 2015; Mittal et al. 2015; Elgamily et al. 2018; Singer et al. 2020; Kurt et al. 2021). Other antimicrobial additives to the powder such as *Cetrimide (CT) and Cetylpyridinum Chloride (CPC)* while *Benzalkonium Chloride (BC)* was tried as an additive to the liquid ((Palenik et al. 1992; Kurt et al. 2021). It was reported by Kurt et al that the added antimicrobial agents may have reduced the fluoride ion release ((Kurt et al. 2021). Antibiotics such as ciprofloxacin and metronidazole were also added (Mittal et al. 2015) in addition to elements as zinc oxide nanoparticles (ZnO-NP) and cerium oxide nanoparticles (CeO2-NP). Moreover, natural products such as Salvadora Persica extract (miswak) (El-Tatari et al. 2011), epigallocatechin-3-gallate (EGCG) (Hu et al. 2013), thyme, cinnamon (Sherief et al. 2021) and propolis were also added to GIC but miswak did not produce antibacterial action (Elgamily et al. 2018).

Among the tried natural products, chitosan, is a nontoxic linear biopolymer produced by partial deacetylation of chitin with many amino groups attached to the polysaccharide main chain that are readily available for chemical reaction and salt formation with acids (Ibrahim et al. 2015; Aliasghari et al. 2016; Divya et al. 2017; Elbahrawy and Abdel Rahim 2017; Mulder and Anderson-Small 2019; Marawan El Azzazy et al. 2021; Soygun et al. 2021). Chitosan possesses weak basic chemical character and shows water and organic solutions insolubility but, shows solubility in diluted water-based acids such as acetic acid. Modifying the liquid phase of a conventional GIC with 10% v/v chitosan significantly improved the antibacterial property of GIC against *S. mutans* as well as its adhesion to enamel and dentin(Ibrahim et al. 2015; Debnath et al. 2017). Chitosan, and its nanoparticles possessed antibacterial characteristics against oral streptococci owing to its positive charge adherence to the bacterial cell wall and membrane rendering them highly bacteriostatic and bactericidal against Gram +ve bacteria such as *S. mutans*, *S.sanguis*, *S. mitus* and *S. salivarius* responsible for caries induction (Ibrahim et al. 2015; Mishra et al. 2017; Wassel and Khattab 2017).

The rationale of the work was to overcome the compromised antibacterial activity of GIC. Therefore, this study aimed to evaluate the effect of adding chitosan nanoparticles as a powder to conventional glass ionomer cement on the antibacterial effect and fluoride ion release. The null hypothesis stated that the antibacterial action and fluoride release of nanochitosan-modified GIC regarding would not be different from conventional GIC.

Methods[1]:

1. Chitosan Nanoparticles preparation

Nanochitosan was produced using methodology conducted by Giftania et al. An amount of 1.5 g. of chitosan powder (Sigma Aldrich, USA) (table 1) dissolved in 250 ml of 2% acetic acid solution was kept under vigorous stirring for 30 min. Then, 0.8 g. of Sodium triphosphate pentabasic purum (STP) (Sigma Aldrich, USA) (table 1) was dissolved in 110 ml of bi-distilled water and added dropwise to the dissolved chitosan and stirred for 60 min. A milky-colored emulsion-like appearance of chitosan nanoparticles is formed. The formed nanoparticles are centrifuged (centrifuge; Hermle Z 200A, Germany) with a maximum speed at 5000 rpm min. The centrifuged chitosan nanoparticles were washed with bi-distilled water three times and dried at 60ºC for 24 hrs using a drying oven (Giftania et al. 2018).

2. Preparation of chitosan nanoparticles modified GIC powder:

Chitosan nanoparticles powder was added as 10 % w/w to conventional GIC powder (GC Gold glass ionomer high strength posterior restorative, Japan) (table 1). The weight percent of added chitosan was determined according to the results of the performed pilot study which revealed the highest antibacterial effect for the group with this percentage (10% w/w). For preparing chitosan nanoparticles modified GIC, 20 mg of chitosan nanoparticles powder was weighed by digital balance and added to 180 mg of glass ionomer powder to obtain the desired percentage 10 % wt / wt of the experimental chitosan nanoparticles modified glass ionomer cement for the sample(Senthil Kumar et al. 2017)**.** Size range of chitosan nanoparticles was determined using Transmission Electron Microscope (TEM- JEOL JEM-2100) where the powder was dispersed in ethanol before imagining (Hembram et al. 2016).

3. Characterization using Fourier transform infrared spectroscopy (FTIR) analysis:

FTIR Spectrometer (Bruker FTIR Spectrometer ALPHA II) was used at a wave-length range of *400 - 4000 cm^{-1}* to analyze functional groups in the GIC powder, GIC liquid, powder of set mass of conventional GIC, purchased chitosan powder, prepared chitosan nanoparticles and powder of set mass of chitosan modified GIC (Senthil Kumar et al. 2017).

Preparation of FTIR samples:

For the powder particles, an amount of 0.40-0.50 mg of the powder sample was ground with 300 mg of KBr powder in the mortar then vacuumed for 5 min and pressed under 10 ton/cm^2 for 15 min to produce a pellet. For the liquid samples, two highly polished salt plates of KBr were prepared with placing a drop of liquid in between them (Shepel et al. 2017). An IR spectrum was obtained by FTIR spectrometer spectrum at a wavelength between 400 cm^{-1} to 4000 cm^{-1}.

4. Sample size calculation:

Based upon the results of a pilot study of the antibacterial test of the two groups (10% and 20 % w/w of nanochitosan-modified GIC) with 5 specimens per group, the effect size (Partial Eta Squared values) for repeated measures ANOVA were 0.597 for groups effects, 0.933 for effect of time and 0.585 for the interaction between the two variables. Using alpha (α) level of (5%) and Beta (β) level of (20%), i.e. power = 80%; the minimum estimated sample size was a total of 9 specimens per group (n=9) for every test. The size of the sample was calculated using G*Power Version 3.1.9.2. The tested groups were as follows:

Intervention group: Nanochitosan modified GIC (10% w/w chitosan nanoparticles added to powder)

[1] Ethics committee approval no. 19-3-15 on 26/3/2019 by the Ethical Committee of Faculty of Dentistry, Cairo University.

Control group: Conventional GIC.

5. Samples Preparation:

The powder/liquid were proportioned in accordance with instructions given by the manufacturer for the conventional cement of glass ionomer. For the intervention group, the pre-weighed powder mixture of chitosan and GIC powders in 10% w/w was mixed with the GIC liquid in the same ratio determined by the manufacturer for conventional GIC to prepare the samples.

6. Direct contact test for antibacterial activity:

Streptococcus mutans strains were grown on *brain heart infusion (BHI)* agar at 37°C for 24 hours in 5% CO_2 to form a suspension and then injected individually into a tube containing 5 ml of sterile saline. The bacterial suspension prepared turbidity was adjusted by comparison against 0.5 McFarland standards = $1.5x10^8$ colony-forming units (CFU) spectrophotometrically at 630 nm. The mixed conventional GIC and nanochitosan-modified GIC (n=18) were applied as a coating on the walls of the wells in the microplates with an equal amount. After 10 min, 10 µl of the prepared bacterial suspension was applied to the coated wells then incubated for one hour in humidity at 37 °C. Afterwards, evaporation of the suspension liquid was done guaranteeing direct contiguity between the tested material's surface and the *Streptococcus mutans* strains. Each of these wells in the microplates was filled with 245 ml of *Brain Heart Infusion broth (BHI).* and mixed for 2 min gently then transferred to adjacent wells containing fresh media (BHI, 215 ml) and incubated at 37 °C. It was carefully avoided that the substance would run to the bottom of the well since that would obstruct the light's route through the microplate well and result in erroneous readings. Optical density measurements were read every hour for 6, 24, 48 and 72 hours in each well (An ELISA Reader Thermo Labsystems Multiskan, China) at 630 nm (Hugar et al. 2016; Kurt et al. 2021).

7. Fluoride ion release test:

The nanochitosan-modified glass ionomer cement and conventional one groups were prepared into Teflon molds of 5 mm height and 8 mm diameter to obtain disc specimens (n=9). Dental floss was inserted into the soft cement to facilitate handling of the samples during immersion in the tested medium (deionized water) then let them to set at 37 °C and 100 % relative humidity for 24 hours. All samples were removed from the Teflon molds and suspended vertically inside plastic bottles containing 5 ml of deionized water and then incubated at 37 °C so they did not adhere to the bottle walls allowing proper wetting of the samples. The deionized water was collected after one day, 7, 14, 21 and 28 days intervals and replaced with fresh water in the same amount and the samples were dried on filter paper and replaced with the same amount of fresh deionized water. The collected solution was buffered with equivalent volumes of TISAB II (total ionic strength adjustor, pH 5.0) and stirred for 30 sec to supply a constant background ionic strength, decomplex fluoride and adjust solution pH. Electrodes were applied in the solution and left for stabilization of the reading. Evaluation of the concentration of the fluoride released in different time periods was carried out and recorded in parts per million (ppm) after each interval (Senthil Kumar et al. 2017; Nishantine et al. 2022).

Statistical Analysis Method:

All variables were represented using mean, standard deviation (SD). Normality of data was approved using Kolmogorov–Smirnov. Independent t-test was applied to compare between the two groups of specimens of nanochitosan modified GIC and conventional GIC. Repeated Measures Analysis of Variance was used to assess changes across different time points within each group and followed by post hoc comparisons with Bonferroni correction. P-value was adjusted by multiplying the uncorrected p-value by the number of comparisons made to set a significance level at 0.05. [(1)] Data were analyzed using IBM SPSS software package version 25.0 (Armonk, NY: IBM Corp).

Results

Particle size of nanochitosan powder:

Transmission electron micrograph (figure 1) showed that the size of chitosan particles ranges from 19 nm to 47 nm with an average of 33 nm.

FTIR analysis of conventional GIC:

Characteristic bands of powder due to SiO_2 were detected at *724.92 cm^{-1}* and *454.08 cm^{-1}*. The FTIR spectrum for GIC polyacrylic acid liquid revealed peaks at *3378 cm^{-1}*, *1704 cm^{-1}*, *1409 cm^{-1}*, *1239 cm^{-1}*, *1134 cm^{-1}*, and *571 cm^{-1}* for the characteristic functional groups *stretching of O-H*, *stretching of C=O*, *stretching of C-O*, *O-H bond*, *Tartaric acid* and *C-H* stretch respectively (table 2). For the set conventional GIC, peaks appeared at *1588 cm^{-1}*, *1455 cm^{-1}* and *1408 cm^{-1}*. These absorption peaks are due to the *asymmetric stretching of strontium polyacrylate*, *asymmetric stretching of aluminum polyacrylate*, and *asymmetric stretching of calcium polyacrylate* respectively (figure 2A) (Young et al. 2004)(Talal et al. 2009; Senthil Kumar et al. 2017; de Oliveira et al. 2019).

FTIR analysis of nanochitosan-modified GIC:

The characteristic functional groups for prepared chitosan nanoparticles were *3492.36 cm^{-1}*, *3086 cm^{-1}*, *1546 cm^{-1}* and *524 cm^{-1}* contributed to *O-H stretch*, *C-H stretch*, *N-O-P stretching vibration* and *P-O bending vibration* respectively (table 3). The band *1546 cm^{-1}* showed that ammonium was crosslinked with the triphosphate. The set mass of the modified group revealed characteristic peaks *2354 cm^{-1}* and *2167 cm^{-1}* credited to *N=C=O stretch* and *C≡N stretching* in addition to *1592 cm^{-1}*, *1455 cm^{-1}* and *1406 cm^{-1}* representing *asymmetric stretching of strontium*, *aluminum* and *calcium polyacrylates* respectively (figure 2B) (Queiroz et al. 2015; Divya et al. 2017; Ayodele et al. 2018; Lustriane et al. 2018).

Antibacterial activity

Nanochitosan-modified GIC and conventional GIC showed bacterial inhibition manifested by their lower mean values of optical density. Each group showed significant increase in antibacterial activity over the time interval of 72 hours. On comparing the two groups, there was no difference between the two groups in the first three hours, but follow-up for 72 hours nanochitosan-modified GIC exhibited significantly higher antibacterial activity (P value <0.0001) (figure 3).

Fluoride ion release

The results showed significantly higher fluoride ion release for nanochitosan-modified GIC group at each of the tested time intervals compared to the conventional GIC group (p- value <0.0001). For conventional GIC, the amount of fluoride released significantly increased after one week compared to 24 hours and no change in the amount released on the 2nd week, followed by a significant decrease in the release on the 3rd week with no change on the 4th week. For nanochitosan-modified GIC, the amount of fluoride release significantly increased after one week compared to 24 hours. The first week has a significant increase in the released amount of fluoride followed by a decrease in fluoride release in the 2nd, 3rd and 4th weeks (figure 4).

Discussion

The present study aimed to improve the antibacterial properties of glass ionomer cement that served well for ART with the advantages of binding to the tooth structure chemically, antibacterial effect and anticariogenicity with an acceptable translucency (Najeeb et al. 2016). Chitosan possesses inherent properties of being nontoxic, biocompatible, biodegradable and cationic with some biological effects like antibacterial and antifungal properties (Wassel and Khattab 2017). Chitosan nanoparticles were chosen as an additive to GIC powder to promote antibacterial effect as it showed improved mechanical properties proved by Kumar et al. in a study that had several limitations and recommended further investigations (Senthil Kumar et al. 2017).

The ionotropic gelation method, as described by several authors, was used to produce nanochitosan. (Giftania et al. 2018; Lustriane et al. 2018). It is a simple and cheap, physical cross-linking method, that avoids using toxic reagents, decreases the undesirable effects and improves biocompatibility compared to other methods.

Table (1): Materials used in the study

Materials	Composition	Manufacturer	Batch number
Conventional glass ionomer cement (GC Gold glass ionomer high strength posterior restorative 1-1 Minipack)	**Powder** Fluoroaluminosilicate, Strontium glass. **Liquid:** Polyacrylic acid, polycarboxylic acid, tartaric acid and water.	GC Corporation, Tokyo, Japan	N 002578 Shade A3
Medium molecular weight chitosan	75-85% Deacetylated chitin, Poly (D-glucosamine).	SIGMA-ALDRICH, USA	448877
Sodium triphosphate pentabasic purum P.a > 98 % (T)	$Na_5P_3O_{10}$	SIGMA-ALDRICH, USA	72061

Table (2): FTIR bands of GIC fluoroaluminosilicate powder and polycarboxylic acid liquid

GIC Powder				GIC Liquid			
Peak	**Interpretation**	**Peak**	**Interpretation**	**Peak**	**Interpretation**	**Peak**	**Interpretation**
3443	O-H stretch	3378	O-H stretch	2008	C≡C stretching	1134	Tartaric acid
1633.46	C=O stretching	2958	O-H stretch	1704	C=O stretch	1087	Tartaric acid
1003.04	SiO_2	2568	O-H stretch	1635	C=O stretch	571	C-H stretching
724.92	SiO_2	2216	C≡C bond	1409	C-O stretching	460	C-H stretching
454.08	SiO_2	2042	C≡C stretching	1239	O-H bond	444	C-H stretching
						420	C-H stretching

Table (3): FTIR bands of chitosan powder and nanochitosan powder particles

Chitosan powder		Nanochitosan powder particles	
Peak	**Interpretation**	**Peak**	**Interpretation**
3437.30	N-H stretching	3492.36	N-H stretch
2875.56	C-H asymmetric stretching	3086.44	C-H stretch
1659.57	N-H bending	2926.43	C-H stretch
1426.21	CH_2 bending	1634.83	C=O/NH_2
1383.46	C-H bending	1546.41	N-O-P stretching vibration
1324.32	C-N stretching	1384.93	C-H stretch
1252.40	C-O stretching	1093.12	C-O stretch
1155.98	C-O-C stretch	1151.74	CN stretch
1027.79	C-N stretching	893.11	C=C bending
900.02	C=C bending	524.31	P-O bending vibration
679	Alkyne C-H bend		
605.72	C-H stretch		

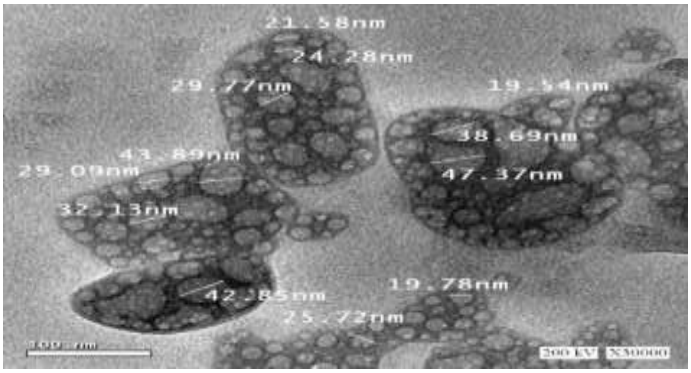

Figure (1): TEM of synthesized nanochitosan (average crystal size 33 nm)

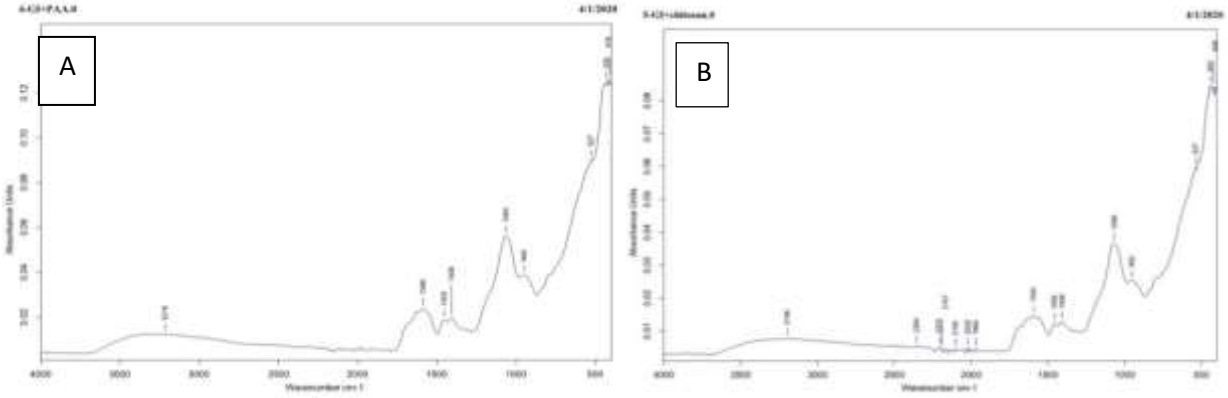

Fig. (2) FTIR spectra of tested groups: A. Set mass of conventional GIC B. Set mass of nanochitosan modified GIC

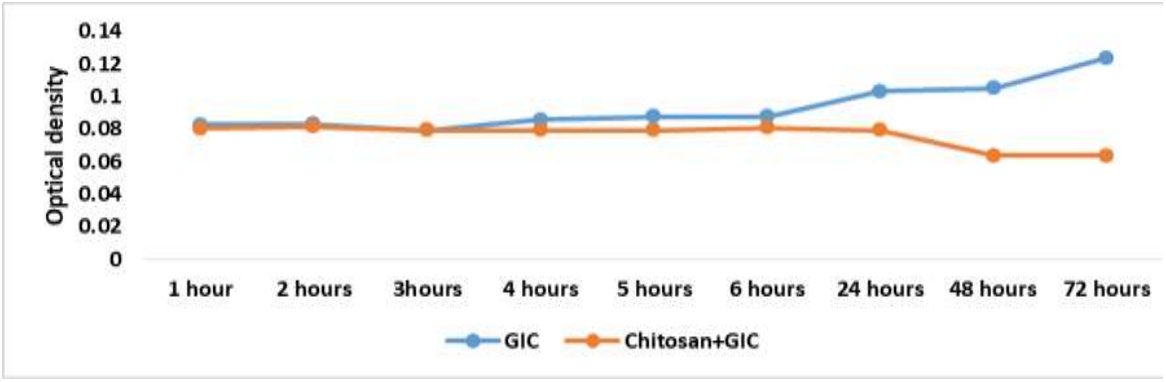

Fig. (3) Optical density values for the antibacterial activity test of the tested groups at different time intervals.

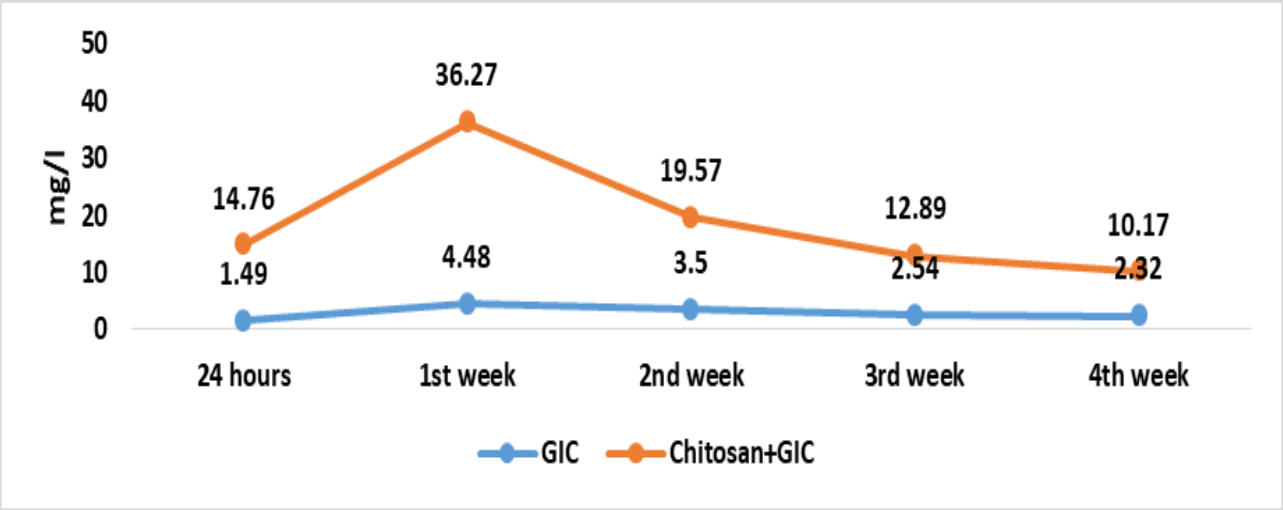

Figure (4): Fluoride ion release of nanochitosan modified GIC and conventional GIC groups at different time intervals

Chitosan is a cationic polysaccharide, forms complex compounds with multivalent anions such as tripolyphosphate (TPP) (Lustriane et al. 2018) whereas the used polyphosphate in our study was STP. The polyphosphoric groups of STP interacted with ammonium groups of chitosan thus enhancing inter and intramolecular interaction imparting a low particle size in nanoscale (Divya et al. 2017; Ayodele et al. 2018; Lustriane et al. 2018) Although nanoochitosan and its bulk counterpart, chitosan, had the same chemical structure, smaller particles possessed distinct physicochemical or electromagnetic properties, which explained the differences in the spectrum bands of FTIR compared to the bulk counterparts (Khan et al. 2018).

Regarding the chemical characterization for conventional GIC by FTIR, the characteristic bands of polyacrylic acid at *1635 cm^{-1}* and *1409 cm^{-1}* that represented *C=O* and *C–O stretching* respectively denoting COOH group were replaced by *1455 cm^{-1}*, *1588 cm^{-1}* and *1408 cm^{-1}* that referred to *C=O asymmetric stretching of aluminum polyacrylate*, *strontium* and *calcium polyacrylate* respectively indicating setting by the formation of crosslinked polysalt network (Young et al. 2004)(Talal et al. 2009; de Oliveira et al. 2019).

On comparing chitosan to nanochitosan, the peak at *3437 cm^{-1}* that contributed to *–NH_2* and *–OH* groups stretching vibration slightly shifted to *3492 cm^{-1}* in nanochitosan indicating that the hydrogen bonding is enhanced (Senthil Kumar et al. 2017). The appearance of *N-O-P stretching* vibration at *1546 cm^{-1}* in nanochitosan can be attributed to the interaction between NH_3^+ groups of chitosan and phosphate groups of STP. The peak at *524 cm^{-1}* in nanochitosan was characteristic *P-O bending vibration* from phosphate groups (Divya et al. 2017; Senthil Kumar et al. 2017; Lustriane et al. 2018).

The set nanochitosan modified GIC revealed a different peak at *3196 cm^{-1}* indicating *N-H stretch/O-H stretch* that can be attributed to an interaction between nanochitosan and GIC through many hydroxyl groups and acetamide groups of nanochitosan capable of binding to hydroxyl groups of the GIC particles and polyacrylic acid (PAA) carboxyl groups via hydrogen bonding (Ibrahim et al. 2015; Debnath et al. 2017). The appearance of characteristic peaks *1592 cm^{-1}*, *1455 cm^{-1}* and *1406 cm^{-1}* representing *asymmetric stretching of strontium*, *aluminum* and *calcium polyacrylates* respectively indicated setting of GIC without any interference from chitosan.

Antibacterial activity of chitosan appeared only in an acidic medium which was related to its poor

solubility at high pH which is considered advantageous. The distinguished antibacterial activity of chitosan could be explained by different mechanisms: (1) Diffusion of hydrolysis products that interacted with microbial DNA thus, inhibiting the synthesis of mRNA and protein. (2) Inhibition of microbial growth through chelation of nutrients and essential metals by chitosan. (3) Chitosan at the surface of the cell acted as a polymer membrane that hindered nutrients entrance to the cell or as an oxygen barrier that restrained aerobic bacterial growth. (4) Interference of chitosan positive charge with the bacterial negative charge on its surface changing the cell permeability (Hosseinnejad and Jafari 2016).

The findings of the present study (figure 3) revealed similar initial antibacterial action of both groups which declined in the control group in accordance with El azzazy but increased in nanochitosan modified GIC group (Marawan El Azzazy et al. 2021). The decline in antimicrobial action of GIC could be related to its maturation as the fresh mix of low pH depicted a higher antibacterial effect. The superior antimicrobial activity of chitosan nanoparticles was in agreement with Divya et al., Wassel and Khattab, Aliasghari et al. and Ibrahim et al. which could be attributed to catalyzing fluoride release by chitosan and high activity of chitosan nanoparticles as polycationic nanoparticles interact with the negatively charged surface of bacteria with higher affinity (Ibrahim et al. 2015; Aliasghari et al. 2016; Divya et al. 2017; Wassel and Khattab 2017). Moreover, the large surface area and spherical character of chitosan nanoparticles enhanced their antimicrobial activity by tightly adsorbing to the bacterial surface disrupting its membrane and causing leakage of intracellular molecules. Small ions as potassium and phosphate were leached out followed by large molecules like DNA and RNA eventually causing cell death (Divya et al. 2017).

The results (figure 4) showed a significant increase in the fluoride ion release of the modified cement in comparison to the conventional one at all time intervals of the test in agreement with Petri et al. (Petri et al. 2007). The burst phenomenon of fluoride release is attributed to the acid-base setting reaction of GIC in accordance with Nishanthine et al. (Nishantine et al. 2022). Fluoride rapidly dissolved from the surface in the short-term release. Afterward, the release of fluoride slowed down, followed by long-term sustained release through pores and fracture lines in the cement (Suprastiwi and Id 2010; Tiwari et al. 2016; Nishantine et al. 2022).

Nanochitosan-modified GIC showed increased F release on the first week which agreed with Senthil Kumar et al. who tested fluoride release after 7 days. The significant increase in F release exhibited by nanochitosan-modified GIC compared to conventional one could be explained by the catalytic effect of chitosan on the fluoride ion release accelerating the diffusion of fluoride through the GIC. This catalytic effect may be due to the presence of a polymeric network attached firmly with inorganic filler that allowed this diffusion. Moreover, fluoride could be transported in nanochitosan-modified GIC matrix in the form of aluminium fluoride (AlF_2) and calcium fluoride (CaF) (Senthil Kumar et al. 2017). This can also explain the decline in fluoride release detected in the following time intervals for both materials due to the depletion of fluoride resources in disagreement with several studies which detected an increase in release over the tested time intervals up to 4 weeks (Petri et al. 2007; Nishantine et al. 2022). Additionally, the initial burst of fluoride contributed to the antibacterial effect detected in both groups (Tiwari et al. 2016). Therefore, the null hypothesis was rejected due to improved antibacterial activity and fluoride release in nanochitosan-modified GIC compared to conventional GIC.

Conclusion:

Given the limits of this research, adding 10 % w/w of chitosan nanoparticles powder to conventional glass ionomer cement powder can promote anticariogenicity of GIC by enhancing its antibacterial activity against *Streptococcus mutans* and fluoride ion release. Further investigation of the effect of aging on the antibacterial activity, adhesion to tooth and microleakage of

nanochitosan-modified GIC is recommended. Also, antimicrobial efficiency against other cariogenic microorganisms needs assessment.

References

Aliasghari, A., Khorasgani, M.R., Vaezifar, S. and Younesi, H. 2016. *Evaluation of antibacterial efficiency of chitosan and chitosan nanoparticles on cariogenic streptococci: An in vitro study Hydrogen as Clean fuel View project*. Available at: https://www.researchgate.net/publication/303788651.

Ayodele, O., Okoronkwo, A., Olugbenga, O.O., Taiwo, A., Elvis Okoronkwo, A., Oludayo Oluwasina, O. and Olusola Abe, T. 2018. Utilization of blue crab shells for the synthesis of chitosan nanoparticles and their characterization Adsorption Potential of Gliricidia sepium on Disperse Yellow 211 Dye View project Energy-Dispersive X-Ray Spectroscopy: Theory and Application in Engineering and Science, Title of Manuscript (Impact of Grinding Machine on Trace Metal Levels in Soup Condiments) View project Utilization of blue crab shells for the synthesis of chitosan nanoparticles and their characterization. *Article in Songklanakarin Journal of Science and Technology* 40(5), pp. 1043–1047. Available at: https://www.researchgate.net/publication/329944845.

Debnath, A., Kesavappa, S.B., Singh, G.P., Eshwar, S., Jain, V., Swamy, M. and Shetty, P. 2017. Comparative evaluation of antibacterial and adhesive properties of chitosan modified glass ionomer cement and conventional glass ionomer cement: An in vitro study. *Journal of Clinical and Diagnostic Research* 11(3), pp. ZC75–ZC78. doi: 10.7860/JCDR/2017/25927.9593.

Divya, K., Vijayan, S., George, T.K. and Jisha, M.S. 2017. Antimicrobial properties of chitosan nanoparticles: Mode of action and factors affecting activity. *Fibers and Polymers* 18(2), pp. 221–230. doi: 10.1007/s12221-017-6690-1.

Elbahrawy, EmanM.S. and Abdel Rahim, RamyA. 2017. Effect of addition of chitosan on water sorption, solubility and microhardness of glass ionomer cement. *Tanta Dental Journal* 14(3), p. 164. doi: 10.4103/tdj.tdj_26_17.

Elgamily, H., Ghallab, O., El-Sayed, H. and Nasr, M. 2018. Antibacterial potency and fluoride release of a glass ionomer restorative material containing different concentrations of natural and chemical products: An in-vitro comparative study. *Journal of Clinical and Experimental Dentistry* 10(4), pp. e312–e320. doi: 10.4317/jced.54606.

El-Tatari, A., de Soel, J.J., de Gee, A.J., Abou Shelib, M. and Amerongen, W.E. 2011. *Influence of salvadora persica (miswak) extract on physical and antimicrobial properties of glass ionomer cement*.

Giftania, W., Koerniasari, E. and Sri, S.A. 2018. Protective Activity of Chitosan Nanoparticle against Cadmium Chloride Induced Gastric Toxicity in Rat. *Journal of Young Pharmacists* 10(3), pp. 303–307. Available at: DOI: 10.5530/jyp.2018.10.67 [Accessed: 14 November 2022].

Hembram, K.C., Prabha, S., Chandra, R., Ahmed, B. and Nimesh, S. 2016. Advances in preparation and characterization of chitosan nanoparticles for therapeutics. *Artificial Cells, Nanomedicine and Biotechnology* 44(1), pp. 305–314. doi: 10.3109/21691401.2014.948548.

Hosseinnejad, M. and Jafari, S.M. 2016. Evaluation of different factors affecting antimicrobial properties of chitosan. *International Journal of Biological Macromolecules* 85, pp. 467–475. doi: 10.1016/j.ijbiomac.2016.01.022.

Hu, J., Du, X., Huang, C., Fu, D., Ouyang, X. and Wang, Y. 2013. Antibacterial and physical properties of EGCG-containing glass ionomer cements. *Journal of Dentistry* 41(10), pp. 927–934. doi: 10.1016/j.jdent.2013.07.014.

Hugar, S.M., Kukreja, P., Assudani, H.G., Patil, V. and Thakkar, P. 2016. Comparative Evaluation of the Antibacterial Efficacy of Type II Glass Ionomer Cement, Type IX Glass Ionomer Cement, and AMALGOMER™ Ceramic Reinforcement by Modified "Direct Contact Test": An in vitro Study. *International Journal of Clinical Pediatric*

Dentistry 9(2), pp. 114–117. doi: 10.5005/jp-journals-10005-1345.

Ibrahim, M.A., Neo, J., Esguerra, R.J. and Fawzy, A.S. 2015. Characterization of antibacterial and adhesion properties of chitosan-modified glass ionomer cement. *Journal of Biomaterials Applications* 30(4), pp. 409–419. doi: 10.1177/0885328215589672.

Khan, S.A., Khan, S.B., Khan, L.U., Farooq, A., Akhtar, K. and Asiri, A.M. 2018. Fourier transform infrared spectroscopy: Fundamentals and application in functional groups and nanomaterials characterization. In: *Handbook of Materials Characterization*. Springer International Publishing, pp. 317–344. doi: 10.1007/978-3-319-92955-2_9.

Kurt, A., Tüzüner, T. and Baygın 2021. Antibacterial characteristics of glass ionomer cements containing antibacterial agents: an in vitro study. *European Archives of Paediatric Dentistry* 22(1), pp. 49–56. doi: 10.1007/s40368-020-00523-z.

LIMA, R.B.W. e, FARIAS, J.F.G. de, ANDRADE, A.K.M., SILVA, F.D.S. da C.M. e and DUARTE, R.M. 2018. Water sorption and solubility of glass ionomer cements indicated for atraumatic restorative treatment considering the time and the pH of the storage solution. *RGO - Revista Gaúcha de Odontologia* 66(1), pp. 29–34. doi: 10.1590/1981-86372018000100043100.

Lustriane, C., Dwivany, F.M., Suendo, V. and Reza, M. 2018. Effect of chitosan and chitosan-nanoparticles on post harvest quality of banana fruits. *Journal of Plant Biotechnology* 45(1), pp. 36–44. doi: 10.5010/JPB.2018.45.1.036.

Marawan El Azzazy, A., Ali, M.S. and Shaban, A.M. 2021. *Effect of Adding nano titanium Dioxide and Chitosan On Antibacterial, Water Sorption and Solubility of Glass Ionomer Cement*. Available at: www.ijmsdr.org.

Mishra, A., Pandey, R.K. and Manickam, N. 2017. Antibacterial effect and physical properties of chitosan and chlorhexidine-cetrimide-modified glass ionomer cements. *J Indian Soc Pedod Prev* 35(1), pp. 28–33. doi: 10.4103/0970-4388.199224.

Mittal, S., Soni, H., Sharma, D., Mittal, K., Pathania, V. and Sharma, S. 2015. Comparative evaluation of the antibacterial and physical properties of conventional glass ionomer cement containing chlorhexidine and antibiotics. *Journal of International Society of Preventive and Community Dentistry* 5(4), p. 268. doi: 10.4103/2231-0762.161754.

Mulder, R. and Anderson-Small, C. 2019. Ion release of chitosan and nanodiamond modified glass ionomer restorative cements. *Clinical, Cosmetic and Investigational Dentistry* 11, pp. 313–320. doi: 10.2147/CCIDE.S220089.

Najeeb, S. et al. 2016. Modifications in glass ionomer cements: Nano-sized fillers and bioactive nanoceramics. *International Journal of Molecular Sciences* 17(7). doi: 10.3390/ijms17071134.

Nishantine, C. et al. 2022. Evaluation of Fluoride Release in Chitosan-Modified Glass Ionomer Cements. *Int Dent J* . Available at: https://doi.org/10.1016/j.identj.2022.05.005 [Accessed: 14 November 2022].

de Oliveira, B.M.B. et al. 2019. Influence of external energy sources on the dynamic setting process of glass-ionomer cements. *Dent Mater* 35(3), pp. 450–456. Available at: doi: 10.1016/j.dental.2019.01.003 [Accessed: 14 November 2022].

Palenik, C.J., Behnen, M.J., Setcos, J.C. and Miller, C.H. 1992. *Inhibition of microbial adherence and growth by various glass ionomers in vitro*.

Petri, D.F.S., Donegá, J., Benassi, A.M. and Bocangel, J.A.J.S. 2007. Preliminary study on chitosan modified glass ionomer restoratives. *Dental Materials* 23(8), pp. 1004–1010. doi: 10.1016/j.dental.2006.06.038.

Queiroz, M.F., Melo, K.R.T., Sabry, D.A., Sassaki, G.L. and Rocha, H.A.O. 2015. Does the use of chitosan contribute to oxalate kidney stone formation? *Marine Drugs* 13(1), pp. 141–158. doi: 10.3390/md13010141.

Senthil Kumar, R., Ravikumar, N., Kavitha, S., Mahalaxmi, S., Jayasree, R., Sampath Kumar, T.S. and Haneesh, M. 2017. Nanochitosan modified glass ionomer cement with enhanced mechanical properties and fluoride release. *International Journal of Biological Macromolecules* 104, pp. 1860–1865. doi: 10.1016/j.ijbiomac.2017.05.120.

Shepel, D., Goreacioc, T., Lupascu, T., Filippov, M. and Rusu, M. 2017. Method of Infrared Spectra Registration of Activated Carbons in Potassium Bromide Pellets. *Chemistry Journal of Moldova* 10(1), pp. 113–115. doi: 10.19261/cjm.2015.10(1).16.

Sherief, D.I., Fathi, M.S. and Abou El Fadl, R.K. 2021. Antimicrobial properties, compressive strength and fluoride release capacity of essential oil-modified glass ionomer cements—an in vitro study. *Clinical Oral Investigations* 25(4), pp. 1879–1888. doi: 10.1007/s00784-020-03493-0.

Singer, L., Bierbaum, G., Kehl, K. and Bourauel, C. 2020. Evaluation of the antimicrobial activity and compressive strength of a dental cement modified using plant extract mixture. *Journal of Materials Science: Materials in Medicine* 31(12). doi: 10.1007/s10856-020-06455-w.

Soygun, K., Soygun, A. and Dogan, M.C. 2021. The effects of chitosan addition to glass ionomer cement on microhardness and surface roughness. *Journal of Applied Biomaterials and Functional Materials* 19. doi: 10.1177/2280800021989706.

Suprastiwi, E. and Id, E.C. 2010. *ANALYSIS OF FLUORIDE RELEASED FROM GIC AND RMGIC IN SALIVA AND DENTINO-ENAMEL SUBSTANCE*. doi: 10.7454/msk.v13i2.356.

Talal, A., Tanner, K.E., Billington, R. and Pearson, G.J. 2009. Effect of ultrasound on the setting characteristics of glass ionomer cements studied by Fourier Transform Infrared Spectroscopy. *Journal of Materials Science: Materials in Medicine* 20(1), pp. 405–411. doi: 10.1007/s10856-008-3578-z.

Tiwari, S. et al. 2016. Antibacterial activity and fluoride release of glass-ionomer cement, compomer and zirconia reinforced glass-ionomer cement. *Journal of Clinical and Diagnostic Research* 10(4), pp. ZC90–ZC93. doi: 10.7860/JCDR/2016/16282.7676.

Wassel, M.O. and Khattab, M.A. 2017. Antibacterial activity against Streptococcus mutans and inhibition of bacterial induced enamel demineralization of propolis, miswak, and chitosan nanoparticles based dental varnishes. *Journal of Advanced Research* 8(4), pp. 387–392. doi: 10.1016/j.jare.2017.05.006.

Young, A.M., Rafeeka, S.A. and Howlett, J.A. 2004. FTIR investigation of monomer polymerisation and polyacid neutralisation kinetics and mechanisms in various aesthetic dental restorative materials. *Biomaterials* 25(5), pp. 823–833. Available at: https://doi.org/10.1016/S0142-9612(03)00599 [Accessed: 14 November 2022].